

*Regular Article***Outage probability of C-NOMA in relaying network with D2D communication pair**

Anh Le-Thi

Faculty of Information Technology, Hanoi University of Industry, Hanoi, Vietnam

Correspondence: Anh Le-Thi, leanh@hau.edu.vn

Communication: received 11 November 2024, revised 03 December 2024, accepted 10 December 2024

Online publication: 15 December 2024, Digital Object Identifier: 10.21553/rev-jec.390

**Abstract**– This paper considers a cooperative Non-Orthogonal Multiple Access (C-NOMA) network with multiple relays and destination user underlay interference constraints from device-to-device (D2D) users. The selected relay improves the decoding capacity from the base station to multi-users over block Rayleigh fading channels. Three relay selection schemes are proposed, such as the partial relay selection scheme for the first hop (RSFH) and second hop (RSSH) and the maximized decoding capacity by the two-stage relay selection (TSRS). To consider the outage performance of the proposed system, the derivations of the analytical expressions for both relay selection schemes for all destination users are provided, and Monte Carlo Simulations are used to confirm the accuracy of these mathematical analyses. Finally, the effects of system essential parameters such as the number of DF-relay nodes, the fixed-power allocation, perfect/imperfect successive interference cancellation (SIC), and the strength of interference from a D2D pair in various scenarios are investigated.

**Keywords**– Multi-user Non-Orthogonal Multiple Access, decode-and-forward, interference from D2D pair, relay selection.

**1 INTRODUCTION**

As a potential candidate for the incoming future network networks B5G, compared with conventional OMA, NOMA has key advantages such as high bandwidth efficiency, serving huge amounts of mobile data traffic with low latency, user fairness, and higher diversity gain [1, 2]. The fundamental principle of NOMA is serving multiple users in the power domain in which users with poorer channel conditions are allocated more power than users with better channel conditions. Moreover, the receiver is equipped with SIC to help detect the desired signal. SIC enables the user with the strongest signal to be decoded first. After that, the signal of the strongest user is re-encoded and re-modulated and is then subtracted from the composite signal. Then, other weaker signals are decoded using the same procedure. The discussion of resource allocation in NOMA and some future research trends of NOMA for 5G and B5G networks have been considered by researchers in [3]. This special issue presented the benefits and opportunities that NOMA offers, its practical applications, and the principles of cooperative NOMA to 5G and B5G networks. Furthermore, some investigators discussed the principles, key features, advantages, and disadvantages of NOMA and other advanced wireless techniques and provided comprehensive comparisons of the solutions for various aspects such as spectral efficiency, system performance, and receiver complexity [4, 5]. As a potential candidate for future wireless networks, including wireless sensor networks (WSN), especially clustering problems [6], when considering the application of NOMA for WSN and other wireless networks, authors focus on how

to improve the efficiency energy of these networks, interference issues, clustering, and so on [7].

**1.1 Related works**

NOMA for downlink and uplink networks has been introduced in studies in which numerous valuable contributions have considered the performance of such NOMA networks. Particularly, the authors in [8] investigated the performance of NOMA, including the superior performance in terms of ergodic sum rates and outage performance in a cellular downlink with randomly deployed users. Authors in [9] investigated the downlink cooperative NOMA in the relaying energy harvesting network with the effects of hardware impairment. Moreover, in [10], user pairing and power allocation approaches for downlink NOMA for visible light communication systems have been investigated. Later, some authors examined the security efficiency of the NOMA network with a multi-input, multi-output technique using meta-heuristic algorithms [11, 12].

To achieve improved coverage, diversity gains, and better fairness in comparison with conventional NOMA, cooperative power-domain NOMA (C-NOMA) was introduced. In [13] a C-NOMA transmission scheme was considered in 5G systems that could obtain an improved diversity gain for weaker NOMA users and reduce the system's complexity by pairing the user. Authors in [14] presented the concepts of C-NOMA in combination with other wireless techniques in 5G to prove the potential advantages of C-NOMA, such as increased capacity and high energy efficiency. Another study [15] considered the performance of end-to-end C-NOMA in Internet-of-things networks with energy harvesting over Nakagami-m fading channels. These

authors examined the effects of time allocation for EH, transmission power, fading conditions, and the number of IoT devices on their proposed system.

Moreover, authors in [16] solved two optimization problems, including maximizing the minimum secrecy rate of the users and maximizing the sum secrecy rate of the C-NOMA system with imperfect SIC. Contributing to C-NOMA studies, [17] investigated the C-NOMA performance with the maximum energy harvested relay selection method and applied the Deep Convolutional Optimized Neural Network to optimize user power allocation. Furthermore, one of the essential problems in C-NOMA with a relaying network is relay selection, in which the effects of relay selection on the outage performance of Energy harvesting C-NOMA schemes were investigated [18].

Apart from the above research, one exciting trend with developing the internet-of-things and mobile applications as device-to-device (D2D) was the improved capacity. In D2D communication schemes, mobile devices that are closer can communicate directly without transmitting data links to the base station or core network [19]. Later, authors in [20] studied the optimal power allocation of NOMA-enabled D2D communications framework with imperfect SIC. In addition, power allocation for the downlink NOMA with D2D communication was investigated in [21]. The authors discussed open research challenges and proposed some interest directions, including multi-user power allocation, signaling overhead, and interference by D2D pairs that may be studied by the research community soon. Furthermore, another study investigated the uplink NOMA scheme containing normal cellular users and underlay D2D users deploying traditional OMA. In this publication, researchers showed that the influence of interference from the D2D pair leads to outage performance and the ergodic capacity of the uplink NOMA network.

## 1.2 Proposed system model

Based on the above survey and to the best of my knowledge, the publications of the C-NOMA network in multi-DF relaying nodes under interference of the device-to-device pairs are limited. NOMA is still considered a potential candidate for B5G due to its advantages in serving multiple users simultaneously in the same frequency band, significantly improving spectrum efficiency. In addition, the DF protocol enables more reliable transmission by enhancing the signal strength at distant users. However, device-to-device (D2D) interference significantly impacts the system's communication quality, especially in cooperative relay networks. Therefore, this paper proposes the downlink C-NOMA scheme in the DF multi-relaying system with the influence of D2D pairs. The source communicates with multiple users via the help of a relaying network. To enhance the decoding capacity from the base station to multi-users over block-Rayleigh fading channels, three relay selection schemes are proposed: the partial relay selection scheme for the first hop (RSFH)

and second hop (RSSH) and the two-stage relay selection (TSRS). Closed-form expressions for the outage probability (OP) for both relay selection strategies are derived to evaluate the system performance. Moreover, Monte Carlo simulations are used to confirm the accuracy of these mathematical analyses. Finally, the effects of system parameters such as the number of DF-relay nodes, the fixed-power allocation, perfect/imperfect successive interference cancellation (SIC), the strength of interference from the D2D pair, and the position of the relay node in various scenarios are investigated.

Notation:  $\|\cdot\|$  is the Frobenius norm;  $CN(0, \sigma)$  is a complex Gaussian distribution with zero mean and variance  $\sigma$ ; and  $\binom{k}{i} = \frac{k!}{i!(k-i)!}$ .

## 2 DESCRIPTION OF SYSTEM MODEL AND RELAY SELECTION

### 2.1 Description of system model

As shown in Figure 1, a system model of a downlink C-NOMA with multi-users is proposed, where a station (S) broadcasts the data signal to  $K$ -destination users  $U_k$ ,  $k = 1, \dots, K$  via a multi-relaying network underlying the impact of a D2D pair. In addition, the multi-relaying network includes  $M$  single-antenna nodes, denoted as  $R_i$ ,  $i = 1, \dots, M$ , and employs the DF protocol to forward the received signals to destination users. I define  $R_b$  as the best relay chosen by the selecting strategies that assist in communicating between S and the destination users. In my proposed system, the relays and multi-destination users in the NOMA scheme employ the perfect/imperfect SICs to detect the desired signals in which multi-destination users are affected by the communication of a D2D pair.

Without loss of generality, I assume that the distance between destination user 1 ( $U_1$ ) and S is the farthest and the distance from S to User  $K$  ( $U_K$ ) is the nearest. This means that the highest power is allocated to  $U_1$ , and the lowest is allocated to  $U_K$ . All nodes were equipped with a single antenna operating in half-duplex mode and had zero-mean additive white Gaussian noise (AWGN) with the same variance of  $N_0$ .

Throughout this paper, I assume that (i) there are no direct links between S and the multiple destination users, (ii) the channels undergo identically and independently distributed Rayleigh block-fading channels; thus channel gains are exponential random variables (RVs) with the coefficients and distances  $(h_{0i}, d_{0i})$ ,  $(h_{ik}, d_{ik})$  and channel gains, respectively  $g_{0i} = (h_{0i})^2$ ,  $g_{ik} = (h_{ik})^2$ , with parameters  $\lambda_{0i} = (d_{0i})^r$  and  $\lambda_{ik} = (d_{ik})^r$ , where  $r$  is the path-loss exponent, and (iii) local CSI is assumed at the relays while global CSI is assumed at S and the users.

Let  $X$  be an exponential random variable with parameter  $\lambda_X$ , where the probability density function (PDF) and cumulative distribution function (CDF) of  $X$  are



expressed as

$$y_{R_b} = \sum_{i=1}^K \sqrt{P\alpha_i} x_i h_{0b} + n_R, \quad (10)$$

where  $n_R$  is the conversion additive white Gaussian noise (AWGN) at R with  $n_R \sim CN(0, \sigma_R^2)$ . In NOMA, the strongest signal will be decoded first, and other weaker signals are handled as noise, and so the same procedure occurs with the next strongest signal. As a result, the signal-to-interference and noise ratios (SINRs) for users at the selected relay are respectively given by

$$\gamma_{x_1}^{R_b} = \frac{\alpha_1 P g_{0b}}{\sum_{i=2}^K \alpha_i P g_{0b} + \sigma_R^2}, \quad (11)$$

$$\gamma_{x_k}^{R_b} = \frac{\alpha_k P g_{0b}}{\sum_{i=1}^{k-1} \varepsilon_i \alpha_i P g_{0b} + \sum_{i=k+1}^K \alpha_i P g_{0b} + \sigma_R^2}, \quad (12)$$

$$\gamma_{x_K}^{R_b} = \frac{\alpha_K P g_{0b}}{\sum_{i=1}^{K-1} \varepsilon_i \alpha_i P g_{0b} + \sigma_R^2}. \quad (13)$$

The cancellation error term is  $\varepsilon_i$ , representing the remaining portion of the canceled message signal  $i^{th}$ . Because of the DF protocol, the selected relay must first successfully detect each signal. After completely decoding destination users,  $R_b$  will forward the superimposed mixture as  $x_R = \sum_{i=1}^K \sqrt{P_R \alpha_i} x_i$  to the destination users, and the received signal at each user includes the signal from  $R_b$  and the signal from the D2D pair. At destination user  $k$ , the received signal is given by

$$y_{U_k} = \sum_{i=1}^K \sqrt{P\alpha_i} x_i h_k + \sqrt{P_{Dk}} x_{Dk} h_{Dk} + n_k \quad (14)$$

where  $n_k$  is the conversion additive white Gaussian noise (AWGN) at R with  $n_R \sim CN(0, \sigma_k^2)$ .

The SINR for each signal at user  $k$  is expressed as

$$\gamma_{x_1}^{U_k} = \frac{\alpha_1 P_R g_k}{\sum_{i=2}^K \alpha_i P_R g_k + P_{Dk} g_{Dk} + \sigma_k^2}, \quad (15)$$

$$\gamma_{x_{k-1}}^{U_k} = \frac{\alpha_{k-1} P_R g_k}{\sum_{i=1}^{k-2} \tau_i \alpha_i P_R g_k + \sum_{i=k}^K \alpha_i P_R g_k + P_{Dk} g_{Dk} + \sigma_k^2}, \quad (16)$$

$$\gamma_{x_k}^{U_k} = \frac{\alpha_k P_R g_k}{\sum_{i=1}^{k-1} \tau_i \alpha_i P_R g_k + \sum_{i=k+1}^K \alpha_i P_R g_k + P_{Dk} g_{Dk} + \sigma_k^2}. \quad (17)$$

Here, the cancellation error term is  $\tau_i$ , representing the remaining portion of the canceled message signal  $i^{th}$ .

### 3 PERFORMANCE ANALYSIS

The outage probability is the probability that the SINR decreases below a predefined threshold, denoted as  $\gamma$ .

In NOMA cooperative transmission, evaluating the OP performance of the system is enabled by examining the transmission performance of multiple users with threshold  $\gamma_0$ . Thus, in this section, we analyze the outage probability of the proposed system with three relay selection strategies.

#### 3.1 OP analysis for RSFH and RSSH

Because of the NOMA and DF protocols, using the partial relay selection schemes, we denote  $E_0$  as the event that the probability of the selected  $R_b$  node successfully decodes users' signals; hence  $E_0$  can be expressed as

$$E_0 = \overline{OP} = \Pr [\gamma_{x_1}^{R_b} > \gamma_0, \dots, \gamma_{x_k}^{R_b} > \gamma_0, \dots, \gamma_{x_K}^{R_b} > \gamma_0]. \quad (18)$$

By substituting equations (11-13) into (19),  $E_0$  can be given by

$$\begin{aligned} E_0 &= \overline{OP} \\ &= \Pr [\gamma_{x_1}^{R_b} > \gamma_0, \dots, \gamma_{x_k}^{R_b} > \gamma_0, \dots, \gamma_{x_K}^{R_b} > \gamma_0] \\ &= \Pr \left[ \frac{\alpha_1 P g_{0b}}{\sum_{i=2}^K \alpha_i P g_{0b} + P_{Dk} g_{Dk} + \sigma_{R_b}^2} > \gamma_0, \dots, \right. \\ &\quad \left. \frac{\alpha_K P g_{0b}}{\sum_{i=1}^{K-1} \varepsilon_i \alpha_i P g_{0b} + \sigma_{R_b}^2} > \gamma_0 \right] \\ &= \Pr [P g_{0b} \Psi_0 > \sigma_{R_b}^2 \gamma_0], \end{aligned} \quad (19)$$

$$\text{here, } \Psi_0 = \min \left\{ \alpha_1 - \gamma_0 \sum_{i=2}^K \alpha_i, \dots, \alpha_K - \gamma_0 \sum_{i=1}^{K-1} \varepsilon_i \alpha_i \right\}.$$

Define  $E_k$  as the event in which destination user  $k$  detects its signal; the  $E_k$  can be expressed as

$$E_k = \Pr [\gamma_{x_1}^{U_k} > \gamma_0, \dots, \gamma_{x_{k-1}}^{U_k} > \gamma_0, \gamma_{x_k}^{U_k} > \gamma_0]. \quad (20)$$

By substituting equations (15-18),  $E_k$  in (20) can be given by

$$E_k = \Pr [\psi_k P_R g_k > \gamma_0 P_{Dk} g_{Dk} + \sigma_k^2 \gamma_0], \quad (21)$$

here,

$$\begin{aligned} \psi_k &= \min \left\{ \left( \alpha_1 - \gamma_0 \sum_{i=2}^K \alpha_i \right), \dots, \right. \\ &\quad \left. \left( \alpha_k - \gamma_0 \sum_{i=1}^{k-1} \tau_i \alpha_i - \gamma_0 \sum_{i=k+1}^K \alpha_i \right) \right\}. \end{aligned}$$

The probability that destination user  $k$  can exactly detect its signal when both events  $E_0$  and  $E_k$  occur, is  $\Pr [E_0, E_k]$ . Therefore, the outage probability that user  $k$  cannot detect its signal is expressed as

$$OP_k = 1 - \Pr [E_0, E_k]. \quad (22)$$

Combining the expressions of  $E_0$  and  $E_k$ , equation (23)

can be re-written as

$$\begin{aligned}
OP_k &= 1 - \Pr \left[ \psi_k P_R g_k > \gamma_0 P_{Dk} g_{Dk} \right. \\
&\quad \left. + \sigma_k^2 \gamma_0, P_{g_{0b}} \Psi_0 > \sigma_R^2 \gamma_0 \right] \\
&= 1 - \left( 1 - F_{g_{0b}} \left( \frac{\sigma_R^2 \gamma_0}{P \Psi_0} \right) \right) \\
&\quad \times \int_0^\infty \left[ \left( 1 - F_{g_k} \left( \frac{\gamma_0 P_{Dk}}{\psi_k P_R} x + \frac{\sigma_k^2 \gamma_0}{\psi_k P_R} \right) \right) f_{g_{Dk}}(x) \right] dx.
\end{aligned} \tag{23}$$

**Theorem 1.** The OP of user  $k$  for the RSFH and RSSH schemes can be expressed as follows, respectively

$$OP_k^{RSFH} = 1 - \left[ \left( 1 - \left( 1 - \exp \left( -\lambda_0 \frac{\sigma_R^2 \gamma_0}{P \Psi_0} \right) \right)^M \right) \times \lambda_D \frac{\exp \left( -\frac{\lambda_k \sigma_k^2 \gamma_0}{\psi_k P_R} \right)}{\frac{\lambda_k \gamma_0 P_{Dk}}{P_R \psi_k} + \lambda_D} \right] \tag{24}$$

$$\begin{aligned}
OP_k^{RSSH} &= 1 - \frac{\lambda_{Dk}}{\lambda_k \frac{\gamma_0 P_{Dk}}{P_R \psi_k} + \lambda_{Dk}} \\
&\quad \times \exp \left( -\lambda_0 \frac{\sigma_R^2 \gamma_0}{P \Psi_0} - \lambda_k \frac{\sigma_k^2 \gamma_0}{\psi_k P_R} \right)
\end{aligned} \tag{25}$$

*Proof.* See Appendix A.

### 3.2 OP analysis for TSRS

Here, I consider the two-stage relay selection (TSRS) strategy. According to equation (6),  $\Pr[\Omega]$  is obtained as

$$\Pr[\Omega] = \Pr \left[ \begin{array}{l} \frac{\alpha_1 P_{g_{01}}}{\sum_{i=2}^K \alpha_i P_{g_{01}} + \sigma_R^2} \geq \gamma_0, \dots, \\ \frac{\alpha_K P_{g_{01}}}{\sum_{i=1}^{K-1} \varepsilon_i \alpha_i P_{g_{01}} + \sigma_R^2} \geq \gamma_0, \\ \vdots \\ \frac{\alpha_1 P_{g_{0m}}}{\sum_{i=2}^K \alpha_i P_{g_{0m}} + \sigma_R^2} \geq \gamma_0, \dots, \\ \frac{\alpha_K P_{g_{0m}}}{\sum_{i=1}^{K-1} \varepsilon_i \alpha_i P_{g_{0m}} + \sigma_R^2} \geq \gamma_0, \\ \vdots \\ \frac{\alpha_1 P_{g_{0M}}}{\sum_{i=2}^K \alpha_i P_{g_{0M}} + \sigma_R^2} < \gamma_0, \dots, \\ \frac{\alpha_K P_{g_{0M}}}{\sum_{i=1}^{K-1} \varepsilon_i \alpha_i P_{g_{0M}} + \sigma_R^2} < \gamma_0 \end{array} \right] \tag{26}$$

**Lemma:** The probability of the event that a set of relays decode the data successfully from the source is given by

$$\begin{aligned}
\Pr[\Omega] &= \left( 1 - \exp \left( -\frac{\lambda_0 \gamma_0 \sigma_R^2}{P \theta_1} \right) \right)^{M-m} \\
&\quad \times \exp \left( -\lambda_0 \frac{m \sigma_R^2 \gamma_0}{P \theta_1} \right).
\end{aligned} \tag{27}$$

*Proof:* Given in Appendix B

Therefore, the probability  $\Pr[|\Omega| = m]$  is obtained as

$$\begin{aligned}
\Pr[|\Omega| = m] &= \binom{M}{m} \times \Pr[\Omega] \\
&= \binom{M}{m} \left( 1 - \exp \left( -\frac{\lambda_0 \gamma_0 \sigma_R^2}{P \theta_1} \right) \right)^{M-m} \\
&\quad \times \exp \left( -\lambda_0 \frac{m \sigma_R^2 \gamma_0}{P \theta_1} \right),
\end{aligned} \tag{28}$$

and

$$\Pr[|\Omega| = 0] = \left( 1 - \exp \left( -\frac{\lambda_0 \gamma_0 \sigma_R^2}{P \theta_1} \right) \right)^M. \tag{29}$$

The non-outage event is obtained, as user  $k$  can detect the desired signal as

$$\bar{E}_k^{TSRS} = \Pr \left[ \gamma_{x_1}^{U_k} > \gamma_0, \dots, \gamma_{x_{k-1}}^{U_k} > \gamma_0, \gamma_{x_k}^{U_k} > \gamma_0 \right]. \tag{30}$$

Thus, the event that user  $k$  cannot detect its signal is expressed as  $1 - \bar{E}_k^{TSRS}$ .

**Theorem 2.** The outage probabilities of users with the two-stage relay selection (TSRS) strategy are expressed as

✓ If  $\frac{\alpha_1}{\sum_{i=2}^K \alpha_i} \leq \gamma_0$ , the outage probability at  $U_1$  is given by

$$OP_1^{TSRS} = 1.$$

✓ If  $\frac{\alpha_1}{\sum_{i=2}^K \alpha_i} > \gamma_0$  the outage probability at  $U_1$  is expressed as

$$\begin{aligned}
OP_1^{RSTS} &= \left( 1 - \exp \left( -\frac{\lambda_0 \gamma_0 \sigma_R^2}{P \theta_1} \right) \right)^M + \\
&\quad \left[ \binom{m}{M} \left( 1 - e^{-\frac{\lambda_0 \gamma_0 \sigma_R^2}{P \theta_1}} \right)^{M-m} e^{-\lambda_0 \frac{m \sigma_R^2 \gamma_0}{P \theta_1}} \right] \\
&\quad \times \left[ 1 - \frac{\lambda_{D1} e^{-\frac{\lambda_1 \gamma_0 \sigma_1^2}{\left( \alpha_1 - \gamma_0 \sum_{i=2}^K \alpha_i \right) P_R}}}{\frac{\lambda_1 P_{D1} \gamma_0}{\left( \alpha_1 - \gamma_0 \sum_{i=2}^K \alpha_i \right) P_R} + \lambda_{D1}} \right]^M
\end{aligned} \tag{31}$$

✓ If  $\theta_k \leq 0$ , the outage probability at  $U_k$  as  $OP_k^{TSRS} = 1$ ,

✓ If  $\theta_k > 0$ , the outage probability at  $U_k$  is given by

$$\begin{aligned}
OP_k^{RSTS} &= P \left( 1 - \exp \left( -\frac{\lambda_0 \gamma_0 \sigma_R^2}{P \theta_1} \right) \right)^M + \\
&\quad \left[ \binom{m}{M} \left( 1 - e^{-\frac{\lambda_0 \gamma_0 \sigma_R^2}{P \theta_1}} \right)^{M-m} \right] \\
&\quad \times \left[ e^{-\lambda_0 \frac{m \sigma_R^2 \gamma_0}{P \theta_1}} \times \left( 1 - \frac{\lambda_{Dk} e^{-\frac{\lambda_k \sigma_k^2 \gamma_0}{\theta_k P_R}}}{\frac{\lambda_k \gamma_0 P_{Dk}}{\theta_k P_R} + \lambda_{Dk}} \right) \right]
\end{aligned} \tag{32}$$

here,  $\theta_k = \min \left\{ \left( \alpha_1 - \gamma_0 \sum_{i=2}^K \alpha_i \right), \dots, \left( \alpha_k - \gamma_0 \sum_{i=1}^{k-1} \tau_i \alpha_i - \gamma_0 \sum_{i=k+1}^K \alpha_i \right) \right\}$ .

*Proof:* Given in Appendix C

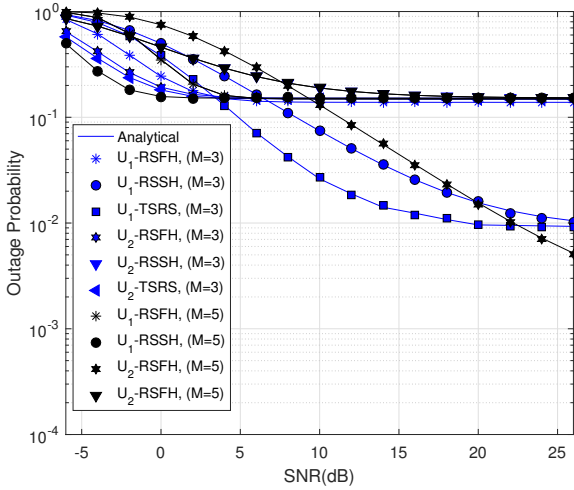


Figure 2. The effect of the number of relay nodes on the outage performance.

#### 4 NUMERICAL RESULTS AND DISCUSSION

In this section, the numerical results and discussion of the outage probability for destination users in the downlink C-NOMA with the impact of a D2D pair for three relay selection strategies are presented via Monte Carlo simulations to validate the analytical expressions given in the above sections. Specifically, the parameters in the proposed system are set as follows: (1) the target data rate,  $R_k = 0.5$  bits/s/Hz; (2) the path loss exponent is set up with a value of 2.7; (3) considering the two-dimensional plane, the coordinates of the S node, R are set to  $(0,0)$ ,  $(d_0,0)$ ; (4) the signal to noise ratio (SNR) at each user is assumed to be the same value and it is defined as  $SNR = P/\sigma^2$ , and the value of noise variance at the relays, destination users, is set as  $\sigma_R^2 = \sigma_1^2 = \sigma_k^2 = \dots = \sigma_K^2 = 0.1$ ; (5) the simulated OMA scheme is compared to the NOMA scheme wherein the total bandwidth is shared equally among destination users. A glance at the figures reveals that the analytical results match the simulation results. A more detailed performance analysis of various cases will be shown below.

Figure 2 presents the effects of the number of relay nodes on OP at  $U_1$  with three relay selection strategies, including RSFH, RSSH, and TSRS, in which two cases are considered,  $M = 3$  and  $M = 5$ . The system parameters are set as follows:  $d_0 = 1$ ,  $d_1 = 1$ ,  $d_2 = 1.2$ , the values of the cancellation error terms at all NOMA users are  $\epsilon = 1\%$ , the power allocation coefficients for each destination user are  $\alpha_1 = 0.7$ ,  $\alpha_2 = 0.3$ , and the interference power from D2D is assumed to be  $SNR_{D2D} = 3$  dB. Generally, as the number of relay nodes increases, the outage performance of both  $U_1$  and  $U_2$  improves with all three relay selection methods. However, the OPs at  $U_1$  with RSFH and  $U_2$  with RSSH are unchanged when the transmit power is high enough, while with TSRS for  $U_1$ , the outage performance is significantly improved, and the system model applying the TSRS method offers the best performance.

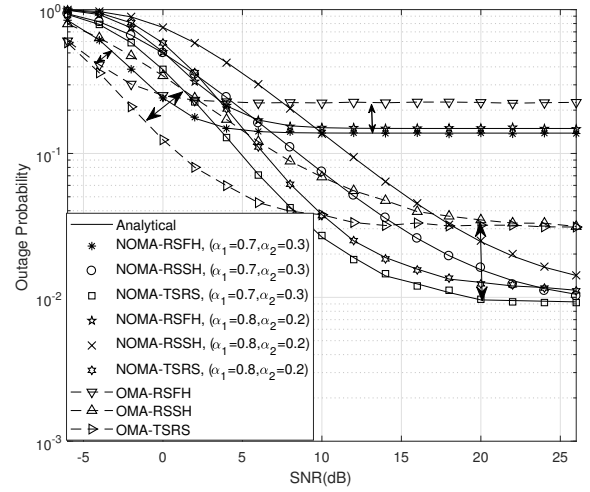


Figure 3. Effects of power allocation coefficients on the outage performance at user 1.

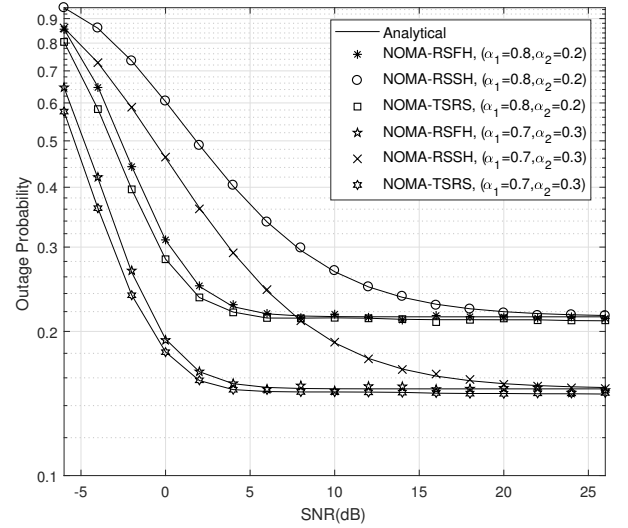


Figure 4. Effects of power allocation coefficients on the outage performance at user 2.

Figure 3 illustrates the outage probability performance at user DU1 of the proposed model for three relay selection methods: RSFH, RSSH, and TSRS. In this case, we consider the proposed system with three relay nodes and two destination users in two cases of power allocation, where the coefficients for each destination user are  $\alpha_1 = 0.7$ ,  $\alpha_2 = 0.3$  and  $\alpha_1 = 0.8$ ,  $\alpha_2 = 0.2$ . The system parameters are set as follows: the distance from selected relay to source and to users are  $d_0 = 1$ ,  $d_1 = 1$ ,  $d_2 = 1.2$  respectively, the values of the cancellation error terms at all NOMA-users as  $\epsilon = 1\%$ , and the interference power from D2D is assumed to be  $SNR_{D2D} = 3$  dB. First, we observe that the trend of OP at  $U_1$  decreases when the transmit power at S increases with three relay selection methods in both the C-NOMA and OMA schemes. In addition, Figure 3 shows that the TSRS relay selection offers the highest performance, while RSFH gives the lowest performance in both the C-NOMA and OMA schemes. Moreover, it is shown that  $U_1$  in the C-NOMA scheme obtains a



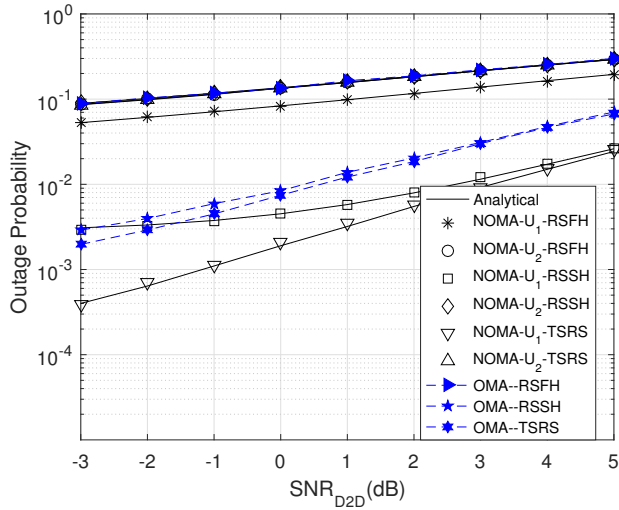


Figure 5. Effects of the D2D pair communication strength on the outage performance.

much better outage probability performance than OMA at high transmit power. In contrast, OMA exhibits better performance at low transmit power. The main reason for this is that in C-NOMA, the transmit power  $P$  is divided into multi-parts for multi-users, thus the smaller the transmit power, the less allocation power for each user in NOMA. As a result, at very low transmit power, the signal strength in C-NOMA compared to OMA is very weak. However, the difference in performance between C-NOMA and OMA at high power is much more than at low power.

Furthermore, Figure 3 shows that the outage probability remains stable when the transmit power is high enough. For example, with RSFH for both C-NOMA and OMA as SNR is greater than approximately 20 dB; with RSSH and TSRS for OMA it is 6 dB. Finally, when  $U_1$  is allocated more power,  $U_1$  in C-NOMA obtains better performance. When the same parameters are set as those in Figure 3,  $U_2$  in Figure 4 has the same trend as the power allocated to  $U_2$  increases, resulting in increased outage performance at  $U_2$ . It can be seen in Figure 4 that  $U_2$  in RSSH obtains the worst performance, whereas RSFH and TSRS offer better performance. Moreover, the case of power allocation for users with  $\alpha_1 = 0.7$ ,  $\alpha_2 = 0.3$  reaches a better performance than the case of  $\alpha_1 = 0.8$ ,  $\alpha_2 = 0.2$ . Thus, we can see that the appropriate power allocation greatly affects the system's quality, which is NOMA's advantage over OMA.

Figure 5 presents the effects of the D2D pair communication strength to OP with both  $U_1$  and  $U_2$ , and three relay selection strategies, including RSFH, RSSH, and TSRS, are also considered. The system parameters are set as follows: the distance from selected relay to and to users are  $d_0 = 1$ ,  $d_1 = 1$ ,  $d_2 = 1.2$  respectively, the values of the cancellation error terms at all NOMA-users are  $\varepsilon = 1\%$ , and the power allocation coefficients for each destination user are  $\alpha_1 = 0.7$ ,  $\alpha_2 = 0.3$ . Figure 5 shows that the greater the interference power of the D2D pair is, the worse the outage performance of the

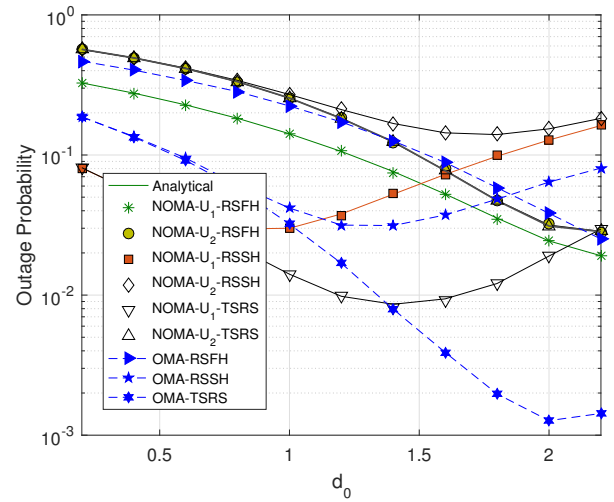


Figure 6. Effects of the position of relaying network on OP on the outage performance.

proposed system. The D2D pair influences the performance of C-NOMA with all relay selection methods.

Figure 6 illustrates the effect of the position of the selected relay on the outage probability with three relay selection methods at a transmitter power  $SNR = 10$  dB. The system parameters are set as follows: the values of the cancellation error terms at all NOMA-users are  $\varepsilon = 1\%$ , and the power allocation coefficients for each destination user are  $\alpha_1 = 0.7$ ,  $\alpha_2 = 0.3$ . It can be seen that the position of the selected relay influences the outage performance of each user with each relay selection strategy. Mainly, with the RSFH method, the trend of OP lines at each user in both C-NOMA and OMA systems is similar in that the further distance the S-R link is, the better the outage performance gets. However, with RSFH and TSRS methods, the OP at users decreases when the distance of the S-R link increases to the threshold. When this distance exceeds the threshold, the OP at users increases, meaning the outage performance is worse. Thus, the relay's position is essential to improve the outage performance of the proposed system. We can see that, for instance, User 1 in the C-NOMA system with the TSRS method obtains the best outage performance at  $d_0 1.4$ , whereas in the OMA system, this values as  $d_0 2$ . Moreover, Figure 6 shows that TSRS offers the best performance compared to RSFH and RSSH methods. Finally, in the case of the lower distance of the S-R link, the C-NOMA system performs better than OMA, and in contrast, the performance of OMA is better than C-NOMA in the case the relay is too far from the source.

## 5 CONCLUSIONS

My paper analyzed the outage performance of a down-link C-NOMA scheme in a multiple DF-relaying network with the impact of interference constraints from a D2D pair over block Rayleigh fading. In my proposed system, three relay selection strategies, RSFH, RSSH, and TSRS, were considered to choose the best relay. This

relay will decode the received signal and forward a mixture of superimposed signals to multi-destination users, assuming that DU1 is far from source S. Moreover, the perfect/imperfect SICs to detect the desired signals were equipped at receivers in the proposed C-NOMA. The analytical expressions for the SOPs of the users with three relaying selection strategies were derived, and their accuracies were validated through Monte Carlo simulations. In addition, the effects of system parameters such as the number of DF-relay nodes, the fixed power allocation, perfect/imperfect successive interference cancelation (SIC), the strength of interference from a D2D pair and the position of the relay node were investigated in various scenarios. These results showed that (1) the NOMA system obtains better secrecy outage performance than the OMA scheme at high enough transmit power; (2) the TSRS scheme obtains the best outage performance, and RSFH gives the worst performance; (3) the number of DF relay nodes increases, the outage performance of the proposed system also increases, especially with the RSSH and TSRS schemes. In future work, I aim to further enhance the system by incorporating Intelligent Reflecting Surface (IRS) technology and Computational Intelligence techniques to significantly improve the system's performance.

## ACKNOWLEDGMENT

This work was supported by the Vietnam National Foundation for Science and Technology Development (NAFOSTED) under Grant 102.02-2023.33.

## REFERENCES

- [1] U. Ghafoor, M. Ali, H. Z. Khan, A. M. Siddiqui, and M. Naeem, "NOMA and future 5G & B5G wireless networks: A paradigm," *Journal of Network and Computer Applications*, vol. 204, p. 103413, 2022.
- [2] M. Ghous, A. K. Hassan, Z. H. Abbas, G. Abbas, A. Hussien, and T. Baker, "Cooperative power-domain NOMA systems: an overview," *Sensors*, vol. 22, no. 24, p. 9652, 2022.
- [3] M. Abd-Elnaby, G. G. Sedhom, E.-S. M. El-Rabaie, and M. Elwekeil, "NOMA for 5G and beyond: literature review and novel trends," *Wireless Networks*, vol. 29, no. 4, pp. 1629–1653, 2023.
- [4] X. Xu, Y. Liu, X. Mu, Q. Chen, H. Jiang, and Z. Ding, "Artificial intelligence enabled NOMA toward next generation multiple access," *IEEE Wireless Communications*, vol. 30, no. 1, pp. 86–94, 2023.
- [5] W. Yi, Y. Liu, and Z. Ding, "Developing NOMA to Next-Generation Multiple Access," in *Fundamentals of 6G Communications and Networking*. Springer, 2023, pp. 291–316.
- [6] M. Raju and K. Lochanambal, "An Insight on Clustering Protocols in Wireless Sensor Networks," *Cybernetics and Information Technologies*, vol. 22, no. 2, pp. 66–85, 2022.
- [7] H. Azarhava, J. M. Niyi, and M. A. Tinati, "NOMA-based energy efficient resource allocation in wireless energy harvesting sensor networks," *Computer Communications*, vol. 209, pp. 302–308, 2023.
- [8] X. Xie, J. Liu, J. Huang, and S. Zhao, "Ergodic capacity and outage performance analysis of uplink full-duplex cooperative NOMA system," *IEEE Access*, vol. 8, pp. 164786–164794, 2020.
- [9] T. A. Le and H. Y. Kong, "Effects of hardware impairment on the cooperative NOMA EH relaying network over Nakagami-m fading channels," *Wireless Personal Communications*, vol. 116, pp. 3577–3597, 2021.
- [10] T. Dogra and M. R. Bharti, "User pairing and power allocation strategies for downlink NOMA-based VLC systems: An overview," *AEU-International Journal of Electronics and Communications*, vol. 149, p. 154184, 2022.
- [11] T. Le Anh and I. P. Hong, "Secrecy performance of a multi-NOMA-MIMO system in the UEH relaying network using the PSO algorithm," *IEEE Access*, vol. 9, pp. 2317–2331, 2020.
- [12] J. Wang, Y. Wang, and J. Yu, "Joint beam-forming, user clustering and power allocation for MIMO-NOMA systems," *Sensors*, vol. 22, no. 3, p. 1129, 2022.
- [13] A. Ahmed, Z. Elsaraf, F. A. Khan, and Q. Z. Ahmed, "Cooperative non-orthogonal multiple access for beyond 5G networks," *IEEE Open Journal of the Communications Society*, vol. 2, pp. 990–999, 2021.
- [14] M. J. Khan and I. Singh, "Cooperative Power-Domain Non-Orthogonal Multiple Access (NOMA) in 5G Systems: Potentials and Challenges," *5G and Beyond Wireless Networks*, pp. 13–36, 2024.
- [15] S. Ghosh, A. Al-Dweik, and M.-S. Alouini, "On the performance of end-to-end cooperative NOMA-based IoT networks with wireless energy harvesting," *IEEE Internet of Things Journal*, vol. 10, no. 18, pp. 16253–16270, 2023.
- [16] I. Amin, D. Mishra, R. Saini, and S. Aïssa, "Power Allocation and Decoding Order Selection for Secrecy Fairness in Downlink Cooperative NOMA With Untrusted Receivers Under Imperfect SIC," *IEEE Transactions on Information Forensics and Security*, 2024.
- [17] M. K. Beuria and S. S. Singh, "Performance analysis of cooperative NOMA with optimized power allocation using deep learning approach," *Wireless Networks*, vol. 30, no. 2, pp. 819–834, 2024.
- [18] Y. Zhou, Y. Zhang, A. A. Khuwaja, Z. Wang, and Q. Zhang, "Analysis of the outage performance of energy-harvesting cooperative-NOMA system with relay selection methods," *Scientific Reports*, vol. 14, no. 1, p. 10732, 2024.
- [19] K. Z. Shen, D. K. So, J. Tang, and Z. Ding, "Power allocation for NOMA with cache-aided D2D communication," *IEEE Transactions on Wireless Communications*, vol. 23, no. 1, pp. 529–542, 2023.
- [20] S. Yu, W. U. Khan, X. Zhang, and J. Liu, "Optimal power allocation for NOMA-enabled D2D communication with imperfect SIC decoding," *Physical Communication*, vol. 46, p. 101296, 2021.
- [21] R. Elouafadi and M. Benjillali, "Cooperative NOMA-based D2D communications: A survey in the 5G/IoT context," in *Proceedings of the 19th IEEE Mediterranean Electrotechnical Conference (MELECON)*. IEEE, 2018, pp. 132–137.



and cyber security.

**Anh Le-Thi** received the B.E. degree in electrical engineering and M.E. degree in information system from Le Quy Don Technical University, Vietnam, in 2011 and 2015, respectively. She also received a Ph.D. degree in the Department of Electrical Engineering at the University of Ulsan, Korea, in 2020. She is a lecturer at Hanoi University of Industry, Hanoi, Vietnam. Her major research interests are wireless communications systems, NOMA communication, physical layer security, IRS,



## APPENDIX A PROOF OF THEOREM 1

This appendix derives the outage probability at users in downlink C-NOMA in a multi-relaying network with the impact of a D2D pair for two relay selection strategies, RSFH and RSSH, in equations (25, 26, 27). According to Equation (24) and substituting Equations in (3a), (1a) and (1b), we have

$$OP_k^{RSFH} = 1 - \left[ \left( 1 - \left( 1 - \exp \left( -\frac{\lambda_0 \sigma_R^2 \gamma_0}{P\Psi_0} \right) \right)^M \right) \lambda_D \times \exp \left( -\frac{\lambda_k \sigma_k^2 \gamma_0}{\psi_k P_R} \right) \times \int_0^\infty \exp \left( -\frac{\lambda_k \gamma_0 P_{Dk}}{P_R \psi_k} x - \lambda_D x \right) dx \right]. \quad (33)$$

Doing the integral in (35), we will obtain the Equation (25). Then, by substituting (3a), (1a) and (1b), for OP at user 1 in RSSH strategy, we have

$$OP_1^{RSSH} = 1 - \lambda_D \left[ \exp \left( -\frac{\lambda_0 \sigma_R^2 \gamma_0}{P\Psi_0} \right) \times \left( \int_0^\infty \exp(-\lambda_D x) dx \right) - \exp \left( -\frac{\lambda_0 \sigma_R^2 \gamma_0}{P\Psi_0} \right) \times \int_0^\infty \left( 1 - \exp \left( -\frac{\gamma_0 \lambda_1 P_{D1}}{P_R \psi_1} x - \frac{\lambda_1 \sigma_k^2 \gamma_0}{\psi_1 P_R} \right) \right)^M \times \exp(-\lambda_D x) dx \right]. \quad (34)$$

Using Newton's binomial formula as the following with  $n \in N$ ,  $(a+b)^n = \sum_{j=0}^n \binom{n}{j} a^{n-j} b^j$ , Equation (36) can be expressed as

$$OP_1^{RSSH} = 1 - e^{-\lambda_0 \frac{\sigma_R^2 \gamma_0}{P\Psi_0}} \lambda_D \times \sum_{j=1}^M \left[ \binom{M}{j} (-1)^{j+1} e^{-\frac{j \lambda_1 \sigma_k^2 \gamma_0}{\psi_1 P_R}} \times \int_0^\infty e^{-\frac{j \lambda_1 \gamma_0 P_{D1}}{P_R \psi_1} x - \lambda_D x} dx \right]. \quad (35)$$

Performing the integral in (37), we obtain Equation (26). With the same method, we get Equation (27) from the below equation

$$OP_k^{RSSH} = 1 - \lambda_{Dk} e^{-\frac{\lambda_0 \sigma_R^2 \gamma_0}{P\Psi_0}} \times \int_0^\infty e^{-\frac{\lambda_k \gamma_0 P_{Dk}}{P_R \psi_k} x - \frac{\lambda_k \sigma_k^2 \gamma_0}{\psi_k P_R}} e^{-\lambda_{Dk} x} dx. \quad (36)$$

This ends the proof of Theorem 1.

## APPENDIX B PROOF OF LEMMA

In this appendix, we calculate equation (29) in lemma. According to (28), we have

$$\begin{aligned} \Pr[\Omega] &= \Pr \left[ \left( \alpha_1 - \gamma_0 \sum_{i=2}^K \alpha_i \right) \min_{j=1,2,\dots,m} \frac{Pg_{0j}}{\sigma_R^2} \geq \gamma_0, \dots, \right. \\ &\quad \left( \alpha_K - \sum_{i=1}^{K-1} \varepsilon_i \alpha_i \right) \min_{j=1,2,\dots,m} \frac{Pg_{0j}}{\sigma_R^2} \geq \gamma_0, \\ &\quad \left( \alpha_1 - \gamma_0 \sum_{i=2}^K \alpha_i \right) \max_{j=m+1,\dots,M} \frac{Pg_{0j}}{\sigma_R^2} < \gamma_0, \dots, \\ &\quad \left. \left( \alpha_K - \sum_{i=1}^{K-1} \varepsilon_i \alpha_i \right) \max_{j=m+1,\dots,M} \frac{Pg_{0j}}{\sigma_R^2} < \gamma_0 \right] \\ &= \Pr \left[ \underbrace{\theta_2 \max_{j=m+1,\dots,M} \frac{Pg_{0j}}{\sigma_R^2} < \gamma_0}_U \leq \theta_1 \underbrace{\min_{j=1,2,\dots,m} \frac{Pg_{0j}}{\sigma_R^2}}_V \right] \\ &= F_U(\gamma_0) (1 - F_V(\gamma_0)). \end{aligned} \quad (37)$$

Considering  $F_V(\gamma_0)$ , we have

$$\begin{aligned} F_V(\gamma_0) &= \Pr \left[ \min_{j=1,2,\dots,m} \frac{Pg_{0j}}{\sigma_R^2} \leq \frac{\gamma_0}{\theta_1} \right] \\ &= 1 - \Pr \left[ \min_{j=1,2,\dots,m} \frac{Pg_{0j}}{\sigma_R^2} > \frac{\gamma_0}{\theta_1} \right] \\ &= 1 - \prod_{j=1}^m \left( 1 - F_{g_{0j}} \left( \frac{\sigma_R^2 \gamma_0}{P\theta_1} \right) \right) \\ &= 1 - \exp \left( -\lambda_0 \frac{m \sigma_R^2 \gamma_0}{P\theta_1} \right). \end{aligned} \quad (38)$$

Considering  $F_U(\gamma_0) = \max_{j=r+1,\dots,M} \frac{Pg_{0j}}{\sigma_R^2}$ , we have

$$\begin{aligned} F_U(\gamma_0) &= \Pr \left[ \max_{j=m+1,\dots,M} g_{0j} \leq \frac{\sigma_R^2 \gamma_0}{P\theta_1} \right] \\ &= \prod_{j=m+1}^M \left( 1 - \exp \left( -\frac{\lambda_0 \gamma_0 \sigma_R^2}{P\theta_1} \right) \right) \\ &= \left( 1 - \exp \left( -\frac{\lambda_0 \gamma_0 \sigma_R^2}{P\theta_1} \right) \right)^{M-m}. \end{aligned} \quad (39)$$

Combining equations (40) and (41), we have  $\Pr[\Omega]$  as in Lemma. This ends the proof of Lemma.

## APPENDIX C PROOF OF THEOREM 2 IN (33, 34)

This appendix derives the outage probability for users in downlink C-NOMA in a multi-relaying network with the impact of a D2D pair for the two-stage relay selection in equations (33, 34). We consider the outage

event at user 1 as

$$\begin{aligned}
 OP_1^{RSTS} &= \Pr \left[ \gamma_{x_1}^{U_1} < \gamma_0 \right] \\
 &= \Pr \left[ \arg \max_{m=1 \dots M} \{ SNR_{i1} \} < \gamma_0 \right] \\
 &= \Pr \left[ \max_{m=1 \dots M} \left\{ \frac{\alpha_1 P_R g_{m1}}{\sum_{i=2}^K \alpha_i P_R g_{m1} + P_{D1} g_{D1} + \sigma_1^2} \right\} < \gamma_0 \right] \\
 &= \prod_{m=1}^M \Pr \left[ \frac{\alpha_1 P_R g_{m1}}{\sum_{i=2}^K \alpha_i P_R g_{m1} + P_{D1} g_{D1} + \sigma_1^2} < \gamma_0 \right] \\
 &= \prod_{m=1}^M \Pr \left[ \left( \alpha_1 - \gamma_0 \sum_{i=2}^K \alpha_i \right) P_R g_{m1} < P_{D1} g_{D1} \gamma_0 + \gamma_0 \sigma_1^2 \right] \quad (40)
 \end{aligned}$$

Because  $\alpha_1 - \gamma_0 \sum_{i=2}^K \alpha_i$  can be positive or negative, we consider the following cases:

✓ In the case  $\frac{\alpha_1}{\sum_{i=2}^K \alpha_i} \leq \gamma_0$ , Equation (42) is expressed as

$$OP_1^{RSTS} = \prod_{m=1}^M \Pr \left[ \frac{\underbrace{\left( \alpha_1 - \gamma_0 \sum_{i=2}^K \alpha_i \right)}_{< 0} P_R g_{m1}}{P_{D1} g_{D1} \gamma_0 + \gamma_0 \sigma_1^2} < \right] = 1 \quad (41)$$

✓ In the case  $\frac{\alpha_1}{\sum_{i=2}^K \alpha_i} > \gamma_0$ , Equation (42) can be expressed as

$$\begin{aligned}
 OP_1^{RSTS} &= \prod_{m=1}^M \left[ \int_0^{+\infty} F_{g_{m1}} \left( \frac{P_{D1} \gamma_0 (\varphi_1)^{-1} x}{\frac{\gamma_0 \sigma_1^2}{P_R} (\varphi_1)^{-1}} \right) f_{g_{D1}}(x) dx \right] \\
 &= \left[ 1 - \lambda_{D1} \left( \frac{\lambda_1 P_{D1} \gamma_0}{P_R} (\varphi_1)^{-1} + \lambda_{D1} \right)^{-1} \right]^M \\
 &\quad \times \exp \left( - \frac{\lambda_1 \gamma_0 \sigma_1^2}{P_R} (\varphi_1)^{-1} \right) \quad (42)
 \end{aligned}$$

here,  $\varphi_1 = \alpha_1 - \gamma_0 \sum_{i=2}^K \alpha_i$ .

In considering the outage probability of other users ( $k=2,3,\dots,K$ ). Denote  $E_k$  is the event that User  $k$  can detect the desired signals with the selected relay, the  $E_k$  can be expressed as follows

$$\begin{aligned}
 E_k &= \Pr \left[ \frac{\alpha_1 P_R g_k}{\sum_{i=2}^K \alpha_i P_R g_k + P_{Dk} g_{Dk} + \sigma_k^2} > \gamma_0, \right. \\
 &\quad \left. \frac{\alpha_k P_R g_k}{\sum_{i=1}^{k-1} \tau_i \alpha_i P_R g_k + \sum_{i=k+1}^K \alpha_i P_R g_k + P_{Dk} g_{Dk} + \sigma_k^2} > \gamma_0 \right] \\
 &= \Pr \left[ P_R g_k \theta_k > \gamma_0 P_{Dk} g_{Dk} + \sigma_k^2 \gamma_0 \right], \quad (43)
 \end{aligned}$$

$$\text{where, } \theta_k = \min \left\{ \left( \alpha_1 - \gamma_0 \sum_{i=2}^K \alpha_i \right), \dots, \left( \alpha_k - \gamma_0 \sum_{i=1}^{k-1} \tau_i \alpha_i - \gamma_0 \sum_{i=k+1}^K \alpha_i \right) \right\}.$$

Thus, the event that User  $k$  cannot detect its signal is given as

$$\begin{aligned}
 OP_k &= 1 - \Pr \left[ \gamma_{x_1}^{U_k} > \gamma_0, \dots, \gamma_{x_{k-1}}^{U_k} > \gamma_0, \gamma_{x_k}^{U_k} > \gamma_0 \right] \\
 &= 1 - \Pr \left[ \theta_k P_R g_k > \gamma_0 P_{Dk} g_{Dk} + \sigma_k^2 \gamma_0 \right]. \quad (44)
 \end{aligned}$$

Because  $\theta_k$  can be positive or negative hence we consider these flowing cases:

✓ In the case of  $\theta_k \leq 0$ , the the event  $OP_k$  can be given by

$$OP_k = 1 - \Pr \left[ > \gamma_0 P_{Dk} g_{Dk} + \sigma_k^2 \gamma_0 \right] = 1 - 0 = 1 \quad (45)$$

✓ In the case of  $\theta_k > 0$ , the event  $OP_k$  can be expressed as

$$\begin{aligned}
 OP_k &= 1 - \Pr \left[ g_k > \frac{\gamma_0 P_{Dk}}{\theta_k P_R} g_{Dk} + \frac{\sigma_k^2 \gamma_0}{\theta_k P_R} \right] \\
 &= 1 - \int_0^{+\infty} \left( 1 - F_{g_k} \left( \frac{\gamma_0 P_{Dk}}{\theta_k P_R} x + \frac{\sigma_k^2 \gamma_0}{\theta_k P_R} \right) \right) f_{g_{Dk}}(x) dx \\
 &= 1 - \int_0^{+\infty} \exp \left( - \frac{\lambda_k \gamma_0 P_{Dk}}{\theta_k P_R} x - \frac{\lambda_k \sigma_k^2 \gamma_0}{\theta_k P_R} \right) \\
 &\quad \times \lambda_{Dk} e^{-x \lambda_{Dk}} dx \\
 &= 1 - \lambda_{Dk} \exp \left( - \frac{\lambda_k \sigma_k^2 \gamma_0}{\theta_k P_R} \right) \\
 &\quad \times \int_0^{+\infty} \exp \left( -x \left( \frac{\lambda_k \gamma_0 P_{Dk}}{\theta_k P_R} + \lambda_{Dk} \right) \right) dx \\
 &= 1 - \frac{\lambda_{Dk}}{\frac{\lambda_k \gamma_0 P_{Dk}}{\theta_k P_R} + \lambda_{Dk}} \exp \left( - \frac{\lambda_k \sigma_k^2 \gamma_0}{\theta_k P_R} \right). \quad (46)
 \end{aligned}$$

Therefore, substituting Equations (46) and (47) into the equation below, we have the outage probability at user  $k$  as in (33, 34).

$$OP_k^{RSTS} = \begin{cases} 1, & \text{if } \theta_k \leq 0, \\ \Pr \left[ |\Omega| = 0 \right] + \sum_{m=1}^M \Pr \left[ |\Omega| = m \right] \times OP_k, & \text{if } \theta_k > 0. \end{cases} \quad (47)$$

This ends the proof of Theorem 2.